

SR-Clustering: Semantic Regularized Clustering for Egocentric Photo Streams Segmentation

Mariella Dimiccoli^{a,c,*}, Marc Bolaños^{a,*}, Estefania Talavera^{a,b}, Maedeh Aghaei^a, Stavri G. Nikolov^d, Petia Radeva^{a,c,**}

^a *Universitat de Barcelona, Barcelona, Spain*

^b *University of Groningen, Groningen, Netherlands*

^c *Computer Vision Center, Barcelona, Bellaterra, Spain*

^d *Imagga Technologies Ltd and Digital Spaces Living Lab, Sofia, Bulgaria*

Abstract

While wearable cameras are becoming increasingly popular, locating relevant information in large unstructured collections of egocentric images is still a tedious and time consuming processes. This paper addresses the problem of organizing egocentric photo streams acquired by a wearable camera into semantically meaningful segments. First, contextual and semantic information is extracted for each image by employing a Convolutional Neural Networks approach. Later, by integrating language processing, a vocabulary of concepts is defined in a semantic space. Finally, by exploiting the temporal coherence in photo streams, images which share contextual and semantic attributes are grouped together. The resulting temporal segmentation is particularly suited for further analysis, ranging from activity and event recognition to semantic indexing and summarization. Experiments over egocentric sets of nearly 17,000 images, show that the proposed approach outperforms state-of-the-art methods.

Keywords: temporal segmentation, egocentric vision, photo streams clustering

1. Introduction

Along with the advances in wearable technology during the last few years, wearable cameras have become more popular. These small light-weight devices allow to discretely capture high quality images in a hands free fashion from a first-person point of view. Wearable video cameras such as GoPro and Loox-cie by having a relatively high frame rate around 35 fps, are mostly used for recording the user experience during a few hours in sports and entertainment.

*Corresponding authors. The first two authors contributed equally to this work.

**Principal corresponding author

Email addresses: mariella.dimiccoli@cvc.uab.es (Mariella Dimiccoli), marc.bolanos@ub.edu (Marc Bolaños), etalavera@ub.edu (Estefania Talavera), maghaeigavari@ub.edu (Maedeh Aghaei), stavri.nikolov@imagga.com (Stavri G. Nikolov), petia.ivanova@ub.edu (Petia Radeva)

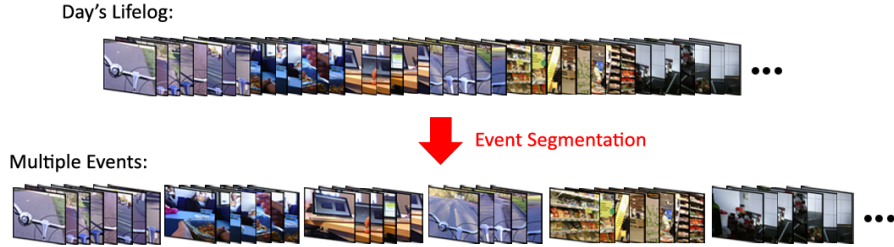


Figure 1: Example of temporal segmentation of an egocentric sequence based on what the camera wearer sees. As it will be seen later, We do not provide a textual description for each segment such as 'street', 'cafeteria', etc., but we do provide a set of semantic attributes that characterize the images of each segment.

Instead, wearable photo cameras, such as the Narrative Clip and SenseCam capture only 2-3 fpm and are therefore mostly used for image acquisition during long periods of time (e.g. a whole day). These data, collected by continuously recording the user life, to understand and track lifestyle behavior, have the potential of enabling the prevention of noncommunicable diseases associated to unhealthy trends and risky profiles (such as obesity, depression, etc.). In addition, used as a tool of re-memory cognitive training, they can be an important tool for prevention or delay of cognitive and functional decline in elderly people [5]. However, egocentric data generally appear in form of long unstructured photo streams of thousands of images, often with high degree of redundancy, from which, the extraction of relevant content is difficult. In addition, abrupt appearance changes are quite frequent even in temporally adjacent frames, requiring robust algorithms for temporal segmentation. These algorithms should not rely solely on low-level features for image representation, but also incorporate semantic information about the events and the environments of the wearer.

This work proposes an unsupervised algorithm that aims to organize egocentric photo streams by grouping temporally adjacent frames into semantically meaningful segments (see Fig. 1). Each segment is aimed to semantically characterize a different event and provide a basis for understanding the semantic structure present in that event. Besides event recognition, the semantic temporal segmentation proposed in this paper, provides a great potential for semantic indexing and browsing.

Early works on egocentric temporal segmentation [3, 25] focused on what the *camera wearer sees*. For this purpose, the authors used as image representation, low-level features to capture the basic characteristics of the environment around the user, such as color, texture or information acquired through different camera sensors. More recently, the works in [18] and [9] have used mid-level features extracted by using the AlexNet model [2] trained on ImageNet as a fixed feature extractor for image representation.

Moreover, some other recent methods focused on what the *camera wearer does* and used as image representation low-level features such as ego-motion

[30, 19, 28, 27] or high-level features as activities [8]. Ego-motion is closely related to the user activity, but temporal segmentation is prone to fail when the environment changes while performing the same kind of motion (e.g. the user is in transit but, first he/she is at home, then he/she is walking in the street and finally, he/she enters to the underground). The same applies to activities. Castro et al. [8] proposed a new approach for temporal segmentation of egocentric photo streams based on classification in a pre-defined set of activities performed by the user. This method combines a specifically trained Convolutional Neural Network (CNN) on egocentric data and a posterior Random Decision Forest in a late-fusion ensemble that obtains promising results for a single user. However, the main problem of this approach is the lack of generalization, needing to re-train the model for any new user, which implies having to manually label large datasets including all the classes to be detected.

To the best of our knowledge, except the work of Castro et al. [8] and our previous work [9], all other state-of-the-art methods have been designed for and tested on videos. In our previous work [9], we proposed an unsupervised method, called *R-Clustering*, that relies on the combination of Agglomerative Clustering (AC), that usually has a high recall, but leads to temporal over-segmentation, with a statistically founded change detector, called ADWIN [1], which is very precise, but, applied to the segmentation problem, usually leads to temporal under-segmentation. Both approaches are integrated in a *Graph-Cut (GC)* [26] framework to obtain a trade-off between AC and ADWIN, which have complementary properties. The graph-cut relies on CNN-based features extracted using AlexNet, trained on ImageNet, as a fixed feature extractor in order to detect the final segments of similar consecutive frames.

In this paper, we extend our previous work by adding a semantic level to the image representation. Due to the Low-Temporal Resolution (LTR) of the camera and to the motion of the camera wearer, temporally adjacent images may present abrupt changes (see Fig. 1 and Fig. 7). Hence, robust techniques are required to group pictures into semantically meaningful temporal segments. Instead of representing images simply by their contextual CNN features, which capture the basic environment appearance, we detect segments as images with the same context represented in terms of semantic visual concepts. Not all semantic concepts in an image are equally discriminant for environment classification: objects like trees and buildings can be more discriminant than objects like dogs or mobile phones, since the former characterizes a specific environment such as forest or street, whereas the latter can be found in many different environments. In this paper, we propose a method called Semantic Regularized Clustering (SR-Clustering), which takes into account semantic concepts in the image together with the global image context. In Fig. 2, the structure of the proposed model can be observed. The proposed method receives as input a photo stream describing the day. First, the contextual and semantic features are extracted to be used for an initial clustering by AC and ADWIN. Graph-Cuts is applied to look for a trade-off between the AC (represented by the bottom coloured circles) and ADWIN (represented by the top coloured circles) approaches. The binary term of the graph-cut imposes smoothness and similar-

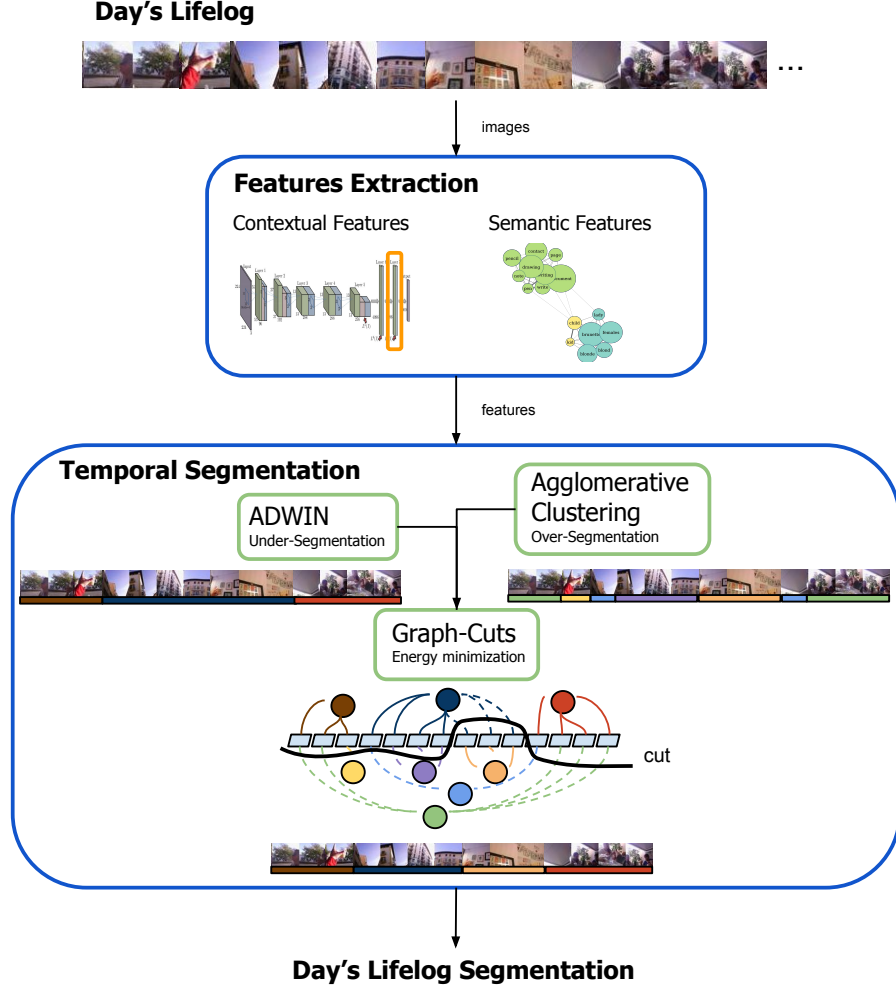


Figure 2: General scheme of the Semantic Regularized Clustering (SR-Clustering) method.

ity of consecutive frames in terms of the CNN image features. The output of the proposed method is the segmented photo stream.

With respect to our previous work, we introduce the following contributions:

- Methodology for egocentric photo streams description based on semantic information.
- Set of evaluation metrics applied to ground truth consistency estimation.
- Evaluation on an extended number of datasets. Including our own, which will be published with this work.

- Exhaustive evaluation on a broader number of methods to compare with.

This manuscript is organized as follows: Section 2 provides a description of the proposed photo stream segmentation approach discussing the semantic and contextual features, the clustering and the graph-cut model. Section 3 presents experimental results and, finally, Section 4 summarizes the important outcomes of the proposed method providing some concluding remarks.

2. Semantic R-Clustering for Temporal Photo Stream Segmentation

In this section, we introduce the semantic and contextual features of SR-clustering and provide a detailed description of the segmentation approach.

2.1. Features

We assume that two consecutive images belong to the same segment if they can be described by similar image features. When we refer to the features of an image, we usually consider low-level image features (color, texture, etc.) or a global representation of the environment (e.g. CNN features). However, the objects or concepts that semantically represent what is happening around the user, also represent different events and can be of high importance for the photo streams segmentation. Below, we detail the features that describe in a semantically rich way the egocentric images, we analyze in our approach.

2.1.1. Semantic Features

Given an image I , let us consider a tagging algorithm that returns a set of objects/tags/concepts detected in the images with their associated confidence. The concept confidence values form a semantic feature vector to be used for the photo streams segmentation. Usually, the number of concepts detected for each sequence of images is large (often, some dozens). On the other hand, there could be a lot of redundancy in the detected concepts due to the presence of synonyms or semantically related words. To manage the semantic redundancy, we will rely on WordNet [21], which is a lexical database that groups English words into sets of synonyms, providing additionally short definitions and word relations.

Given a day’s lifelog, let us cluster the concepts by relying on their synset ID in WordNet to compute their similarity in meaning, and following, apply clustering (e.g. Spectral clustering) to obtain 100 clusters. As a result, we can semantically describe each image in terms of 100 concepts and their associated confidence scores. Formally, we first construct a semantic similarity graph $\mathcal{G} = \{V, E, W\}$, where each vertex or node $v_i \in V$ is a concept, each edge $e_{ij} \in E$ represents a semantic relationship between two concepts, v_i and v_j and each weight $w_{ij} \in W$ represents the strength of the semantic relationship, e_{ij} . We compute each w_{ij} by relying on the meanings and the associated similarity given by WordNet, between each appearing pair. To do so, we use the max-similarity

between all the possible meanings m_i^k and m_j^r in M_i and M_j of the given pair of concepts v_i and v_j :

$$w_{ij} = \max_{m_i^k \in M_i, m_j^r \in M_j} \text{sim}(m_i^k, m_j^r).$$

To compute the Semantic Clustering, we use their similarity relationships in the spectral clustering algorithm to obtain 100 semantic concepts, $|C| = 100$. In Fig 3, a simplified example of the result obtained after the clustering procedure is shown. For instance in the purple cluster, we can see that similar concepts like 'writing', 'document', 'drawing', 'write', etc. are grouped in the same cluster, and 'writing' is chosen as the most representative term. For each cluster, we choose as its representative concept, the one with the highest sum of similarities with the rest of elements in the cluster.

Thus, the semantic feature vector $f^s \in \mathbb{R}^{|C|}$ for image I is a 100-dimensional array, such that each component $f^s(I)_j$ of the vector represents the confidence with which the j -th concept is detected in the image. The confidence value for the concept j , representing the cluster C_j , is obtained as the sum of the confidences r_I of all the concepts included in C_j that have also been detected on image I :

$$f^s(I)_j = \sum_{c_k \in \{C_j\}} r_I(c_k)$$

where C_I is the set of concepts detected on image I , C_j is the set of concepts in cluster j , and $r_I(c_k)$ is the confidence associated to concept c_k on image I . The final confidence values are normalized so that they are in the interval $[0, 1]$.

Taking into account that the camera wearer can be continuously moving, even if in a single environment, the objects that can be appearing in temporally adjacent images may be different. In order to tackle this problem, we apply a Parzen Window Density Estimation method [24] to the matrix obtained by concatenating the semantic feature vectors along the sequence. By applying this further step, we aim to obtain a smoothed and temporally coherent set of confidence values. Additionally, we discard the concepts with a low variability of confidence values along the sequence which correspond to non-discriminative concepts that can appear on any environment. The low variability of confidence value of a concept may correspond to constantly having high or low confidence value in most environments.

In Fig. 4, the matrix of concepts (semantic features) associated to an ego-centric sequence is shown, displaying only the top 30 classes. Each column of the matrix corresponds to a frame and each row indicates the confidence with which the concept is detected in each frame. In the first row, the ground truth of the temporal segmentation is shown for comparison purposes. With this representation, repeated patterns along a set of continuous images correspond to the set of concepts that characterizes an event. For instance, the first frames of the sequence represent an indoor scene, characterized by the presence of people (see examples Fig. 5). The whole process is summarized in Fig. 6.

In order to consider the semantics of temporal segments, we used a concept detector based on the auto-tagging service developed by Imagga Technologies

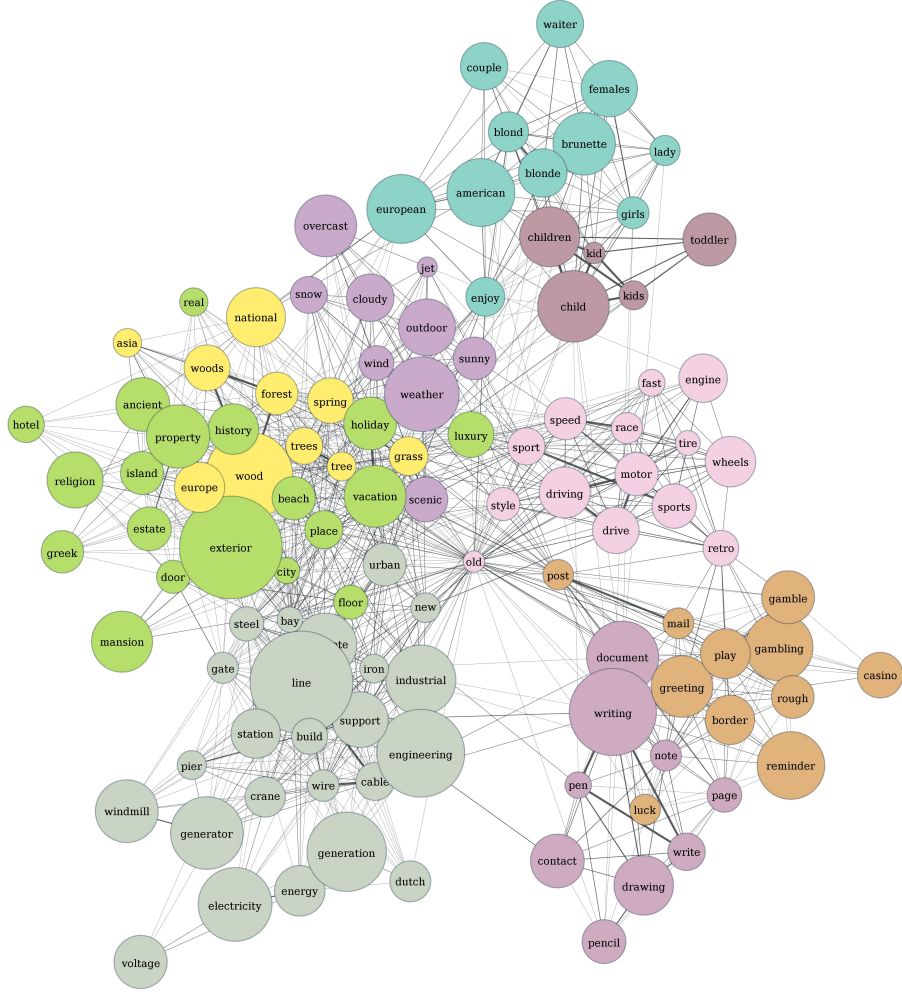


Figure 3: Simplified graph obtained after calculating similarities of the concepts of a day's lifelog and clustering them. Each color corresponds to a different cluster, the edge width represents the magnitude of the similarity between concepts, and the nodes size represents the number of connections they have (the biggest node in each cluster is the representative one). We only showed a small subset of the 100 clusters. This graph was drawn using graph-tool (<http://graph-tool.skewed.de>).

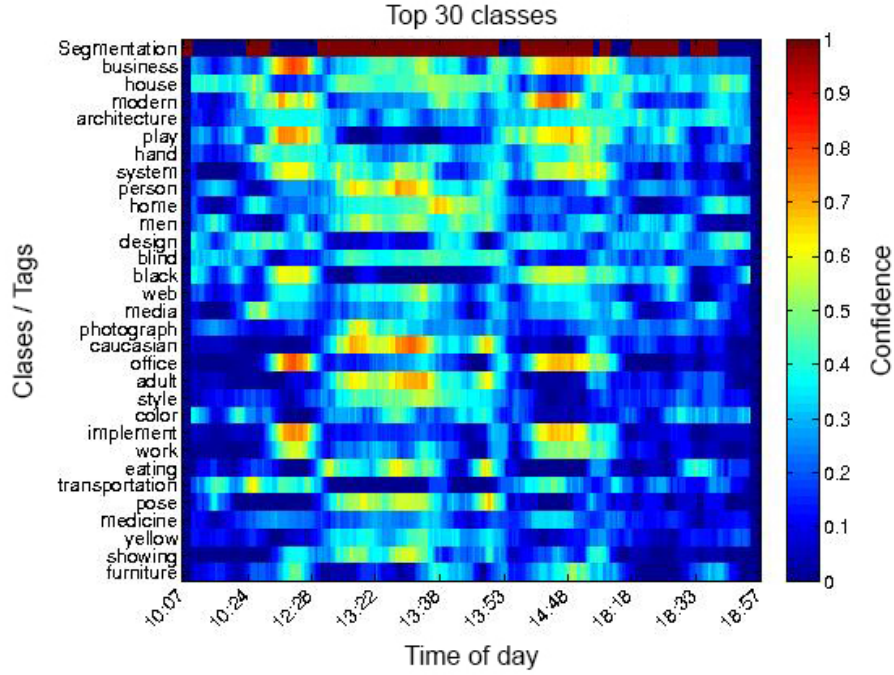


Figure 4: Example of the final semantic feature matrix obtained for an egocentric sequence. The top 30 concepts (rows) are shown for all the images in the sequence (columns). Additionally, the top row of the matrix shows the ground truth (GT) segmentation of the dataset.



Figure 5: Example of extracted tags on different segments. The first one corresponds to the period from 13.22 - 13.38 where the user is having lunch with colleagues, and the second, from 14.48 - 18.18, where he/she is working in the office with the laptop.

Ltd. Imagga's auto-tagging technology ¹ uses a combination of image recognition based on deep learning and CNNs using very large collections of human

¹<http://www.imagga.com/solutions/auto-tagging.html>

to run the CNN. Due to the fact that the weights have been trained on the ImageNet database [12], which is made of images containing single objects, we expect that the features extracted from images containing multiple objects will be representative of the environment. It is worth to remark that we did not use the weights obtained by using a CNN pre-trained on the scenes from Places 205 database [6], since the field of view of the Narrative camera is narrow, which means that most of the time there is not enough field-of-view to characterize the whole scene. Instead, we usually just see objects on the foreground. As detailed in [9], to reduce the large variation distribution of CNN features, which results problematic when computing distances between vectors, we used a signed root normalization to produce more uniformly distributed data [15].

2.2. Temporal Segmentation

The SR-clustering for temporal segmentation is based on fusing the semantic and contextual features with the R-Clustering method described in [9].

2.2.1. Agglomerative Clustering

Once concatenating the semantic and contextual features, the hierarchical agglomerative clustering (AC) method is applied following a bottom-up clustering procedure. In each iteration, the method merges the most similar pair of clusters based on the distances among the image features, updating the elements similarity matrix. This is done until exhausting all possible consistent combinations. The global parameter *cutoff* defines the consistency of the merged clusters. We use the Cosine Similarity between samples, which is suited for high-dimensional positive spaces [23]. The shortcoming of this method is that the final result tends to over-segment the photo streams data.

2.2.2. ADWIN

To compensate the over-segmentation produced by AC, we proposed to model the egocentric sequence as a multi-dimensional data stream and to detect changes in the mean distribution through an adaptive learning method called ADWIN [1], which provides a rigorous statistical guarantee of performance in terms of false positive rate. The method, based on the Hoeffding’s inequality [11], tests recursively if the difference between the averages of two temporally adjacent (sub)windows of the data, say W_1 and W_2 , is larger than a threshold. The value of the threshold takes into account if both sub-windows are *large enough* and *distinct enough* for a k -dimensional signal [20], computed as:

$$\epsilon_{cut} = k^{1/p} \sqrt{\frac{1}{2m} \ln \frac{4}{k\delta'}}$$

where p indicates the p -norm, $\delta \in (0, 1)$ is a user defined confidence parameter, and m is the harmonic mean between the lengths of W_1 and W_2 . In other words, given a predetermined confidence, ADWIN statistically guarantees that it will find any major change in the data means. Given a confidence value δ , the higher the dimension k is, the more samples n the bound needs to reach

assuming the same value of ϵ_{cut} . The higher the norm used is, the less important the dimensionality k is. Since we model the sequence as a high dimensional data stream, ADWIN is unable to predict changes involving a relatively small number of samples, which often characterizes LTR egocentric data, leading to under-segmentation. Moreover, since it considers only the mean change, it is unable to detect changes due to other statistics such as the variance.

2.2.3. Graph-Cuts regularization

We use Graph-Cuts (GC) as a framework to integrate both of the previously described approaches, AC and ADWIN, finding a compromise between them and that at the same time naturally produces a temporally consistent result. GC is an energy-minimization technique that works by finding the minimum of an energy function usually composed of two terms: the *unary term* U , also called data term, that describes the relationship of the variables to a possible class and the *binary term* V , also called pairwise or regularization term, that describes the relationship between two neighboring samples (temporally close images) according to their feature similarity. The binary term smooths boundaries between similar frames, while the unary term keeps the cluster membership of each sequence frame according to its likelihood. In our problem, we defined the unary term as the sum of 2 parts ($U_{ac}(f_i)$ and $U_{adw}(f_i)$). Each of them expresses the likelihood of an image I_i represented by the set of features f_i to belong to segments coming from the corresponding previously applied segmentation methods. The energy function to be minimized is the following:

$$E(f) = \sum_i^n \left[(1 - \omega_1)U_{ac}(f_i) + \omega_1 U_{adw}(f_i) \right] + \omega_2 \sum_i^n \left[\frac{1}{|N_i|} \sum_{j \in N_i} V_{i,j}(f_i, f_j) \right]$$

where $f_i = [f^c(I_i), f^s(I_i)]$, $i = \{1, \dots, n\}$ are the set of contextual f^c and semantic image features f^s for the i -th image, N_i is a set of temporal neighbours centered at i , and ω_1 and ω_2 ($\omega_1, \omega_2 \in [0, 1]$) are the unary and the binary weighting terms, respectively. We can improve the segmentation outcome of GC by defining how much weight do we give to the likelihood of each unary term and balancing the trade-off between the unary and the pairwise energies, respectively. The minimization is achieved through the max-cut algorithm, leading to a temporal segmentation with similar frames having as large likelihood as possible to belong to the same segment, while maintaining segment boundaries in temporally neighboring images with high feature dissimilarity.

More precisely, the unary energy is composed of two terms representing, each of them, the likelihoods of each sample to belong to each of the clusters (or decisions) obtained either applying ADWIN (T_{adw}) or AC (T_{ac}) respectively:

$$U_{ac}(f_i) = P_{ac}(f_i \in T_{ac}), \quad U_{adw}(f_i) = P_{adw}(f_i \in T_{adw})$$

The pair-wise energy is defined as:

$$V_{i,j}(f_i, f_j) = e^{-\text{dist}(f_i, f_j)}$$

An illustration of this process is shown in Fig. 2.

3. Experiments and Validation

In this section, we discuss the datasets and the statistical evaluation measurements used to validate the proposed model and to compare it to state-of-the-art methods. To sum up, we apply the following methodology for validation:

1. We used 3 datasets acquired by 3 different wearable cameras.
2. As statistical measure to compare the final results of different methods, we used the F-Measure.
3. We applied two consistency measures to compare different manual segmentations.
4. We compare SR-Clustering with 3 state-of-the-art techniques.
5. We validate the different components of SR-Clustering to prove the robustness of the final proposal.

3.1. Data

To evaluate the performance of our method, we used 3 public datasets (AIHS, EDUB-Seg and Huji EgoSeg’s sub dataset) acquired by three different wearable cameras.

EDUB-Seg: For this work, we have constructed a new dataset recorded by the Narrative Clip². Our Narrative dataset, named EDUB-Seg (Egocentric Dataset of the University of Barcelona - Segmentation), contains a total of 10 days recorded by 5 different users, making a total of 6,618 images.

AIHS: is a subset of the daily images from the database called *All I Have Seen* (AIHS) [22], recorded by the SenseCam camera. We selected 5 days from their dataset by following the order and amount of images per day that they define in their main website, making a total of 9,320 images. Comparing both cameras (Narrative and SenseCam), we can remark their difference with respect to the lens, they use (fish eye vs normal), and the quality of the images, they record. Additionally, SenseCam acquires images with a larger field of view and significant deformation and blurring. We manually defined the GT for this dataset following the same criteria, we used for the EDUB-Seg photo streams.

Huji EgoSeg: Due to the lack of other publicly available LTR datasets for event segmentation, we also test our temporal segmentation method to the ones provided in the dataset Huji EgoSeg [28]. This dataset was acquired by the GoPro camera, which captures videos with a temporal resolution of 30fps. Considering the very significant difference in frame rate of this camera compared to Narrative (2 fpm) and SenseCam (3 fpm), we applied a sub-sampling of the data by just keeping 2 images per minute, which makes it comparable to the other datasets. In this dataset, several short videos recorded by two different users are provided. Consequently, after sub-sampling all the videos, we merged the resulting images from all the short videos to construct a dataset per user, making a total of 700 images. The images were merged following the numbering

²<http://getnarrative.com/>

order, the authors gave to their videos. We manually defined the GT for each of the two datasets following the same criteria, we used for the EDUB-Seg pictures.

In summary, we evaluate the algorithms on 17 days with a total of 16,638 images recorded by 8 different persons. All datasets contain a mixture of highly variable indoor and outdoor scenes with a large variety of objects. We will make public the EDUB-Seg dataset³, together with our GT segmentations of the datasets Huji EgoSeg and AIHS. Additionally, we release the SR-Clustering ready-to-use complete code⁴.

3.2. Experimental setup

Following [29], we measured the performances of our method by using the F-Measure (FM) defined as follows:

$$FM = 2 \frac{RP}{R + P},$$

where P is the precision defined as ($P = \frac{TP}{TP+FP}$) and R is the recall, defined as ($R = \frac{TP}{TP+FN}$). TP , FP and FN are the number of true positives, false positives and false negatives of the detected segment boundaries of the photo stream. We define the FM, where we consider TPs the images that the model detects as limits or boundaries of an event and that were close to the boundary image defined in the GT by the annotator (given a tolerance of 5 images). The FPs are the images detected as events delimiters, but that were not defined in the GT, and the FNs the lost boundaries by the model that are indicated in the GT. Lower FM values represent a wrong boundary detection while higher values indicate a good segmentation. Having the ideal maximum value of 1, where the segmentation correlates completely with the one defined by the user.

The annotation of temporal segmentations of photo streams is a very subjective task. The fact that different users usually do not perform the same when annotating may lead to bias in the evaluation performance. The problem of the subjectivity when defining the ground truth was previously addressed by [7] in the context of image segmentation. In that work, the authors proposed two measures to compare different segmentations of the same image. They used these measures to validate if segmentations performed by different people were consistent and this able to serve as an objective benchmark for the evaluation of the segmentation performances. In Fig. 7, we report a visual example that illustrates the need of this measure for temporal segmentation of egocentric photo streams. For instance, the scene in the street is split in different segments when analysed by different subjects even if there is a degree of consistency among all splits. Inspired by this work, we re-define the local refinement error, between two temporal segments, as follows:

$$E(S_A, S_B, I_i) = \frac{|R(S_A, I_i) \setminus R(S_B, I_i)|}{|R(S_A, I_i)|},$$

³The link to the dataset will be released on the final version of the article.

⁴<https://github.com/MarcBS/SR-Clustering/releases/tag/src>

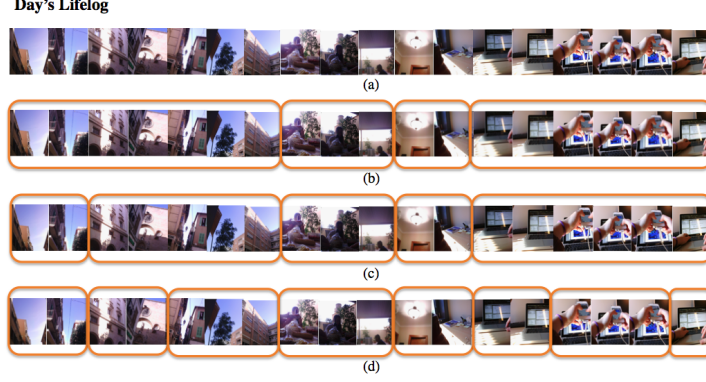


Figure 7: Different segmentation results performed by different subjects. (a) shows a part of a day. (b), (c) and (d) are examples of the segmentation performed by three different persons. (c) and (d) are refinements of the segmentation performed by (b). All three results can be considered correct, since segmentation is an intrinsic subjective task. As a consequence, a metric should not penalize different, but still consistent results of the segmentation.

where \setminus denotes the set difference, S_A and S_B are the two segmentations to be compared. $R(S_X, I_i)$ is the set of images corresponding to the segment that contains the image I_i , when obtaining the segmentation boundaries S_X .

If one temporal segment is a proper subset of the other, then the images lie in an interval of refinement, and the local error should be zero. However, if there is no subset relationship, then, the two regions overlap in an inconsistent manner and the local error should be non-zero. Based on the definition provided, two error measures are defined by combining the values of the local refinement error for the entire sequence. The first error measure is called Global Consistency Error (GCE) and forces all local refinements to be in the same direction (segments of segmentation A can be only local refinements of segments of segmentation B). The second error measure is the Local Consistency Error (LCE), which allows refinements in different directions in different parts of the sequence (some segments of segmentation A can be of local refinements of segments of segmentation B and vice versa). The two measures are defined as follows:

$$GCE(S_A, S_B) = \frac{1}{n} \min \left\{ \sum_i^n E(S_A, S_B, I_i), \sum_i^n E(S_B, S_A, I_i) \right\}$$

$$LCE(S_A, S_B) = \frac{1}{n} \sum_i^n \min \{ E(S_A, S_B, I_i), E(S_B, S_A, I_i) \}$$

where n is the number of images which composes the sequence, S_A and S_B are the two different temporal segmentations and I_i indicates the i -th image of the sequence. The GCE and LCE measures produce output values in the range $[0, 1]$ where 0 means no error.

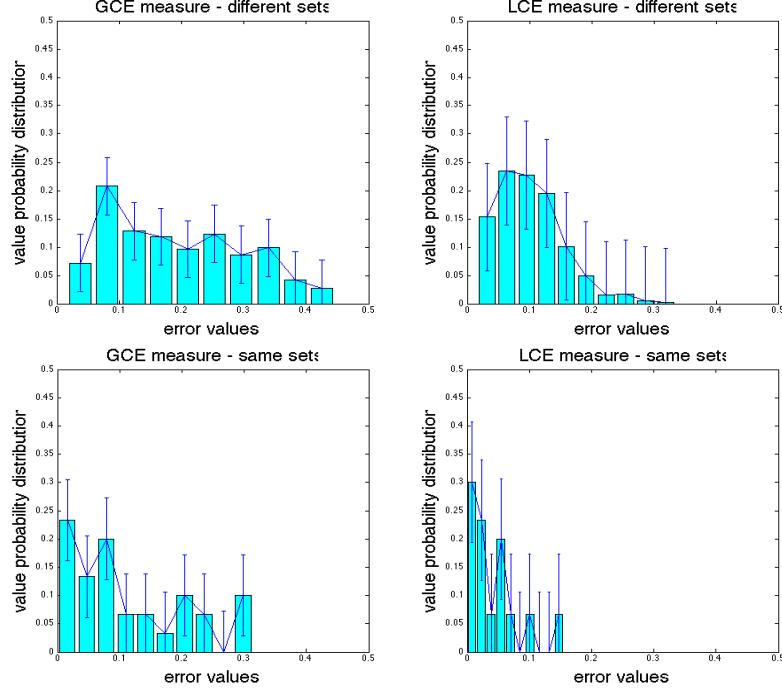


Figure 8: GCE (left) and LCE (right) normalized histograms with the error values distributions, showing their mean and variance. The first row graphs represent the distribution of errors comparing segmentations of different sequences while the second row graphs show the distribution of error when comparing segmentations of the same set.

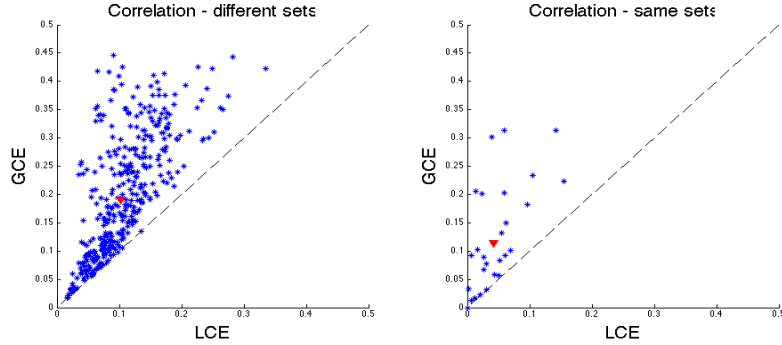


Figure 9: LCE vs GCE for pairs of segmentations of different sequences (left) and for pairs of segmentations of the same sequence (right). The differences w.r.t. the dashed line $x=y$ show how GCE is a stricter measure than LCE. The red dot represents the mean of all the cloud of values.

We asked three different users to segment each of the 10 sets of the EDUB-Seg dataset resulting in 30 different segmentations. The number of all possible

pairs of segmentations is 435, 30 of which are pairs of segmentations of the same set. For each pair of segmentations, we computed GCE and LCE. First, we considered only pairs of segmentations of the same sequence and then, considered the rest of possible pairs of segmentations in the dataset. The first two graphics in Fig. 8 (first row) show the GCE (left) and LCE (right) when comparing each set segmentations with the segmentations applied on the rest of the sets. The two graphics in the second row show the distributions of the GCE (left) and LCE (right) error when analyzing different segments describing the same video. As expected, the distributions that compare the segmentations over the same photo stream have the center of mass to the left of the graph, which means that the mean error between the segmentations belonging to the same set is lower than the mean error between segmentations describing different sets.

In Fig. 9 we compare, for each pair of segmentations, the measures produced by different datasets segmentations (left) and the measures produced by segmentations of the same dataset (right). In both cases, we plot LCE vs. GCE. From the plots, we see what we were expecting, that GCE is higher in all the cases (all values are situated above the line), and that LCE and GCE are describing similar qualities of the segmentation.

As it is shown, the average error between segmentations of the same photo stream (right) is lower than the average error between segmentations of different photo streams (left). Therefore, from this experiment, we can conclude that given the task of segmenting an egocentric photo stream into events, different people tend to produce consistent and valid segmentation.

When comparing the different segmentation methods w.r.t. the obtained FM (see section 3.3), we applied a grid-search for choosing the best combination of hyper-parameters. The set of hyper-parameters (which are only applicable to the corresponding methods) and the ranges tested are the following:

- AC linkage methods $\in \{ward, centroid, complete, weighted, single, median, average, \}$
- AC cutoff $\in \{0.2, 0.4, \dots, 1.2\}$,
- GraphCut unary weight ω_1 and binary weight $\omega_2 \in \{0, 0.1, 0.2, \dots, 1\}$,
- AC-Color $t \in \{10, 25, 40, 50, 60, 80, 90, 100\}$.

3.3. Experimental results

In Table 1 we show the FM results obtained for each segmentation or clustering method on the different datasets. The first two columns correspond to the datasets already used in [9] (AIHS and the first half of EDUB-Seg, Set1), and the third and fourth columns correspond to the newly added half of EDUB-Seg (Set2) and the results of the complete EDUB-Seg (always with the optimal combination of parameters).

In the first section of the table, we evaluated methods proposed in other papers on our datasets. The first one is the Motion-Based segmentation algorithm proposed by Bolaños et al. [19]. As can be seen, the average results obtained



Figure 10: Illustration of our SR-Clustering segmentation results from a subset of pictures from a Narrative set. Each line represents a different segment. Below each segment we show the top 8 concepts found (from left to right). Only a few pictures from each segment are shown.

are far below SR-Clustering. This is because the features used in this method are suited for applying a motion-based segmentation, which is more oriented to activities, and is not always fully aligned with the event segmentation labeling that we consider in our approach (i.e. in an event where the user goes outside from his/her workplace, and then enters to the underground tunnels can be considered "in transit" by the Motion-Based segmentation, but be considered as three different events in our event segmentation). Furthermore, the obtained FM score on the Narrative datasets is lower than the SenseCam's for several reasons: Narrative has lower frame rate compared to Sensecam (AIHS dataset), which is a handicap when computing motion information, and the images have less blur and motion information. We also evaluated the proposal of Lee and Grauman [16], where they apply an Agglomerative Clustering segmentation us-

	AIHS [22]	EDUB-Seg Set1	EDUB-Seg Set2	EDUB-Seg
AC-Color [16]	0.60	0.37	0.61	0.49
Motion [19]	0.66	0.34		
RC [9]	0.79	0.55		
ADW	0.31	0.32		
ADW-ImaggaD	0.35	0.55	0.32	0.43
AC	0.68	0.45		
AC-ImaggaD	0.72	0.53	0.76	0.64
SR-Clustering-LSDA	0.78	0.60	0.77	0.64
SR-Clustering-NoD	0.77	0.66	0.7	0.64
SR-Clustering	0.78	0.69	0.79	0.68

Table 1: Average FM result for each of the tested methods on the egocentric datasets. RC stands for R-Clustering, ADW for ADWIN, ImaggaD is our proposal of semantic features, where D stands for Density Estimation.

ing LAB color histograms. In this case, we see that the algorithm is even far below the result obtained by AC, where the Agglomerative Clustering algorithm is used, but using contextual CNN features instead of colour. The main reason for this performance difference comes from the high difference in features expressiveness, that supports the necessity of using a rich set of features for correctly segmenting highly variable egocentric data. On the last row of this section, we can see the results obtained by our previously published method [9], where we were able to outperform the state-of-the-art of egocentric segmentation using contextual CNN features both on AIHS and on EDUB-Seg Set1. Another clear proposal to compare with would be the one from Castro et al. [8], although they do not provide their CNN for applying this comparison.

In the second part of the Table 1, we compare the results obtained using only ADWIN or only AC with (ADW-ImaggaD, AC-ImaggaD) and without (ADW, AC) semantic features. One can see that using the proposed semantic features, leads to an improved performance, indicating that these features are rich enough to provide improvements on egocentric data segmentation.

Finally, on the last part of Table 1, we compared the segmentation methodology using different definitions for the semantic features. In the SR-Clustering-LSDA case, we used a simpler semantic features description, formed by using the concepts extraction method proposed in [13]. In the last two lines, we tested the model using our proposed semantic methodology (Imagga’s tags) either without Density Estimation, SR-Clustering-NoD or with the final Density Estimation (SR-Clustering), respectively. Comparing the results of the first two rows, we can see that our method is able to outperform the results on EDUB-Seg Set1 adding 14 points of improvement to the FM score, while keeping nearly the same value on the SenseCam dataset. For the later, the FM score slightly falls due to the lower quality of pictures and, thus, the associated higher difficulty to reliably detect semantic concepts. The improvement achieved using semantic

information can also be corroborated, when comparing the FM scores obtained on the second half of EDUB-Seg dataset (Set2 on the 3rd column) and on the complete version of this data (on the last column).

	Huji EgoSeg [28]	LTR
ADW-ImaggaD		0.59
AC-ImaggaD		0.88
SR-Clustering	- - - - -	0.88

Table 2: Average FM score for each of the tested methods using our proposal of semantic features on the dataset presented in [28].

In Table 2 we report the FM score obtained by applying our model on the Huji EgoSeg dataset sub-sampled for being comparable to LTR cameras. We were able to obtain a very high performance, getting 0.88 of FM for both AC and SR-Clustering when using our proposed semantic features. The clear improvement when using the GoPro camera w.r.t. Narrative or SenseCam can be explained by two key factors: 1) the stability of the images when the device is worn mounted on a helmet, and 2) the higher image quality achieved by this kind of camera. The disadvantages come from the facts of: 1) not being capable of acquiring images from the whole day due to battery and memory constraints, and 2) being more obtrusive for the user wearing on a helmet or head in real applications.

In addition to the FM score, we could not consider the GCE and LCE measures to compare the consistency of the automatic segmentations to the ground truth, since both methods lead to a number of segments much larger than the number of segments of the ground truth and therefore these measures would not be meaningful. This is due to the fact that two trivial segmentations achieve error zero for LCE and GCE: any segmentation is a refinement of one segment for the entire sequence, and one image per segment is a refinement of any segmentation. However, we observed that on average, the number of segments obtained by the method of Lee and Grauman [16] is about 4 times bigger than the number of segments, we obtain for the SenseCam dataset and about 2 times bigger than for the Narrative datasets. Indeed, we achieve an higher FM score with respect to the method of Lee and Grauman [16], since it produces a considerable over-segmentation compared to the GT.

3.4. Discussion

The experimental results detailed in section 3.3 have shown the advantages of using more elaborated/semantic features for the temporal segmentation of egocentric photo streams. In spite of the common agreement about the inability of low-level features in providing understanding of the semantic structure present in complex activities or events [10], and the need of semantic indexing and browsing image retrieval system, the use of high level features in the context of egocentric temporal segmentation and summarization has been very limited. This is mainly due to the difficulty of dealing with the huge variability

of object appearance and illumination conditions in egocentric images. In the work of Lee and Grauman [16], devoted to egocentric video summarization, important objects are used to drive the coherence of the summary, while temporal segmentation is still based on classical low level features. In addition to the difficulty of reliably recognizing objects, the temporal segmentation of egocentric photo streams has to cope with the lack of temporal coherence, which in practice means that motion features cannot reliably be estimated. The work of Castro et al. [8] relies on the visual appearance of single images to guess the class/event of an image and on meta-data such as day of the week and hour of the day to regularize over time. However, due to the huge variability in appearance and timing of daily activities, this approach cannot be easily generalized to many different users, implying that for each new user it would be need to label thousand of images for re-training the model.

The method proposed in this paper offers the advantage of being needless of a cumbersome learning stage and offers a better generalization. The concept detector, we used has proved to offer a rich vocabulary to describe the environment surrounding the user. This rich characterization is not only useful for better segmentation of sequences into meaningful and distinguishable events, but could also serve as a tool for event classification or activity recognition among others. For example, Aghaei et al. [17, 4] employed the temporal segmentation method in [9] to extract and select segments with trackable people to be processed. However, incorporating the semantic temporal segmentation proposed in this paper, would allow, for example, to classify events into social or non-social events. Moreover, using additional existing semantic features in a scene may be used to differentiate between different types of a social event ranging from a official meeting (including semantics such as laptop, paper, pen, etc.) to a friendly coffee break (coffee cup, cookies, etc.). Moreover, the semantic temporal segmentation proposed in this paper is useful for indexing and to locate relevant information.

4. Conclusions and future work

This paper proposed an unsupervised approach for the temporal segmentation of egocentric photo streams that is able to partition a day’s lifelog in segments sharing semantic attributes, hence providing a basis for semantic indexing and event recognition. The proposed approach first detects concepts for each image separately employing a CNN approach and later, clusters found concepts taking into account their semantic similarity, hence defining the vocabulary of concepts of a day. Semantic features are combined with global image features capturing more generic contextual information to increase their discriminative power. By relying on these semantic features, a Graph-Cuts technique is used to integrate a statistical bound produced by the concept drift method, ADWIN and the Agglomerative Clustering, two methods with complementary properties for temporal segmentation. We evaluated the performance of the proposed approach on different segmentation techniques and on 17 day sets acquired by

three different wearable devices, and we showed the improvement of the proposed method with respect to the state-of-the-art. Additionally, we introduced two consistency measures to validate the consistency of the ground truth. Furthermore, we made publicly available our dataset EDUB-Seg, together with the ground truth annotation and the code. We demonstrated that the use of semantic information on egocentric data is crucial for the development of a high performance method.

Further research will be devoted to exploit the semantic information that characterizes the segments either for activity or for event recognition, where social events are of special interest. Additionally, we are interested in using semantic attributes to describe the camera wearer context, hence opening new opportunities for developing systems that can take benefit from contextual awareness, including systems for stress monitoring and daily routine analysis.

Acknowledgments

This work was partially founded by TIN2012-38187-C03-01 and SGR 1219. M. Dimiccoli is supported by a *Beatriu de Pinòs* grant (Marie-Curie COFUND action). P. Radeva is partly supported by an *ICREA Academia'2014* grant.

References

References

- [1] R. Gavalda A. Bifet. Learning from time-changing data with adaptive windowing. In *In Proc. SIAM International Conference on Data Mining*, 2007.
- [2] G. E. Hinton A. Krizhevsky, I. Sutskever. Imagenet classification with deep convolutional neural networks. In *Advances in Neural Information Processing Systems*, pages 1097–1105. 2012.
- [3] A. F. Smeaton A. R. Doherty. Automatically segmenting lifelog data into events. In *Proceedings of the 2008 Ninth International Workshop on Image Analysis for Multimedia Interactive Services*, pages 20–23, 2008.
- [4] Maedeh Aghaei, Mariella Dimiccoli, and Petia Radeva. Towards social interaction detection in egocentric photo streams. In *Proceedings of the International Conference on Machine Vision*, 2015.
- [5] Abby C. King et al. Aiden R. Doherty, Steve E. Hodges. Wearable cameras in health: the state of the art and future possibilities. In *American journal of preventive medicine*, volume 44, pages 320–323. Springer, 2013.
- [6] J. Xiao A. Torralba A. Oliva B. Zhou, A. Lapedriza. Learning deep features for scene recognition using places database. In *Advances in Neural Information Processing Systems*, pages 487–495, 2014.
- [7] D. Tal J. Malik D. Martin, C. Fowlkes. A database of human segmented natural images and its application to evaluating segmentation algorithms and measuring ecological statistics. In *In Proc. 8th International Conference on Computer Vision*, pages 416–423, 2001.

- [8] Vinay Bettadapura Edison Thomaz Gregory Abowd Henrik Christensen Daniel Castro, Steven Hickson and Irfan Essa. Predicting daily activities from egocentric images using deep learning. *ISWC*, 2015.
- [9] M. Bolaños M. Aghaei P. Radeva E. Talavera, M. Dimiccoli. R-clustering for egocentric video segmentation. In *Iberian Conference on Pattern Recognition and Image Analysis*. Springer, 2015.
- [10] Amirhossein Habibian and Cees GM Snoek. Recommendations for recognizing video events by concept vocabularies. *Computer Vision and Image Understanding*, 124:110–122, 2014.
- [11] W. Hoeffding. Probability inequalities for sums of bounded random variables. *Journal of the American Statistical Association*, 58(301):pp. 13–30, 1963.
- [12] R. Socher L.-J. Li K. Li L. Fei-Fei J. Deng, W. Dong. Imagenet: A large-scale hierarchical image database. In *In Proc. IEEE Conference on Computer Vision and Pattern Recognition*, pages 248–255, 2009.
- [13] E. S. Tzeng-R. Hu J. Donahue R. Girshick-T. Darrell K. Saenko J. Hoffman, S. Sergio. Lsda: Large scale detection through adaptation. In *Advances in Neural Information Processing Systems*, pages 3536–3544, 2014.
- [14] Y. Jia. Caffe: An open source convolutional architecture for fast feature embedding. <http://caffe.berkeleyvision.org/>, 2013.
- [15] F. He Q. Tian L. Zheng, Sh. Wang. Seeing the big picture: Deep embedding with contextual evidences. *CoRR*, abs/1406.0132, 2014.
- [16] Yong Jae Lee and Kristen Grauman. Predicting important objects for egocentric video summarization. *International Journal of Computer Vision*, 114(1):38–55, 2015.
- [17] P. Radeva M. Aghaei, M. Dimiccoli. Multi-face tracking by extended bag-of-tracklets in egocentric videos. *arXiv preprint arXiv:1507.04576*, 2015.
- [18] E. Talavera X. Giró-i-Nieto P. Radeva M. Bolaños, R. Mestre. Visual summary of egocentric photostreams by representative keyframes. *arXiv preprint arXiv:1505.01130*, 2015.
- [19] P. Radeva M. Bolaños, M. Garolera. Video segmentation of life-logging videos. In *Articulated Motion and Deformable Objects*, pages 1–9. Springer-Verlag, 2014.
- [20] S. Segui C. Malagelada-F. Azpiroz P. Radeva M. Drozdal, J. Vitria. Intestinal event segmentation for endoluminal video analysis. In *In Proc. International Conference on Image Processing*, 2014.
- [21] G. A. Miller. Wordnet: a lexical database for english. *Communications of the ACM*, 38(11):39–41, 1995.
- [22] V. Murino N. Jojic, A. Perina. Structural epitome: a way to summarize one’s visual experience. pages 1027–1035, 2010.
- [23] V. Kumar P. N. Tan, M. Steinbach. *Introduction to Data Mining, (First Edition)*. Addison-Wesley Longman Publishing Co., Inc., Boston, MA, USA, 2005.
- [24] E. Parzen. On estimation of a probability density function and mode. *The annals of mathematical statistics*, pages 1065–1076, 1962.
- [25] A. Hauptmann W.-H. Lin. Structuring continuous video recording of everyday life using time-constrained clustering. In *Proc. SPIE, Multimedia Content Analysis, Management, and Retrieval*, 959, 2006.

- [26] R. Zabih Y. Boykov, O. Veksler. Fast approximate energy minimization via graph cuts. *IEEE Transactions on Pattern Analysis and Machine Intelligence*, 23(11):1222–1239, 2001.
- [27] S. Peleg C. Arora Y. Poley, A. Ephrat. Compact CNN for indexing egocentric videos. *CoRR*, abs/1504.07469, 2015.
- [28] Shm. Peleg Y. Poley, Ch. Arora. Temporal segmentation of egocentric videos. In *In Proc. of the IEEE Conference on Computer Vision and Pattern Recognition*, 2014.
- [29] W. Jia M. Sun Z. Li, Z. Wei. Daily life event segmentation for lifestyle evaluation based on multi-sensor data recorded by a wearable device. In *In Proc. Engineering in Medicine and Biology Society*, pages 2858–2861. IEEE, 2013.
- [30] K. Grauman Z. Lu. Story-driven summarization for egocentric video. In *In Proc. IEEE Conference on Computer Vision and Pattern Recognition*, pages 2714–2721, 2013.